

## PEI-coated Fe<sub>3</sub>O<sub>4</sub> magnetic nanoparticles for fast and segregative removal of uric acid from plasma

Y. Z. Pan<sup>a</sup>, W. H. Wang<sup>b</sup>, Y. Huang<sup>c</sup>, C. X. Yi<sup>d</sup>, X. Huang<sup>d,e\*</sup>

<sup>a</sup>*School of Chemical Engineering, Sichuan University of Science & Engineering, Zigong, Sichuan, 643000, P. R. China*

<sup>b</sup>*School of Kinesiology, Shanghai University of Sport, Shanghai, 200438, P. R. China*

<sup>c</sup>*College of Lab Medicine, Hebei North University, Key Laboratory of Biomedical Materials of Zhangjiakou, Zhangjiakou, Hebei, 075000, P. R. China*

<sup>d</sup>*School of Sports and Health Science, Tongren University, Tongren, Guizhou, 554300, P. R. China*

<sup>e</sup>*School of Physical Education, Guangxi University of Science and Technology, Liuzhou, Guangxi, 545006, P. R. China*

Excess uric acid in blood would cause serious health consequences. Extracorporeal blood purification using solid phase adsorbents is considered as the most promising technique for uric acid removal for patients with nephropathy. In this work, PEI-coated Fe<sub>3</sub>O<sub>4</sub> NPs have been synthesized to be a fast and segregative remover of uric acid. They present a fast and efficient adsorption behavior. Meanwhile, PEI-coated Fe<sub>3</sub>O<sub>4</sub> NPs are magnetic separable and biocompatible. Therefore, PEI-coated Fe<sub>3</sub>O<sub>4</sub> NPs hold a great potential in uric acid removal both in vitro and in vivo.

(Received September 8, 2021; Accepted January 29, 2022)

*Keywords:* Magnetic nanoparticles, PEI, Uric acid, Removal, Segregation

### 1. Introduction

Uric acid is the final product of purine nucleotide catabolism in human body. For healthy people, the production of uric acid is in a dynamic balance. While, when the concentration of uric acid in serum is over 416  $\mu\text{mol/L}$  for men and 357  $\mu\text{mol/L}$  for women, it is can be diagnosed as hyperuricemia<sup>[1]</sup>. Urate would crystallize resulting from the excess residual of uric acid in body and deposit to cause inflammation. This eventually leads to the formation of tophi and occurrence of gout<sup>[2]</sup>. Besides, diabetes, hypertension, nephrolith and angiocardiopathy are the most common complications with serious health consequences<sup>[3]</sup>. Reducing the high purine foods intake<sup>[4]</sup>, administrating drugs to inhibit uric acid synthesis and synthase<sup>[5]</sup>, promote uric acid excretion and alkalify urine are effective way to treat hyperuricemia<sup>[6]</sup>. However, patients with nephropathy who suffer from renal failure or renal insufficiency are difficulty in uric acid excretion. They have to undergo hemodialysis to eliminate uric acid in clinic. Currently, extracorporeal blood purification using solid phase adsorbents is considered as the most promising technique. So far, some adsorbents such as mesoporous silica<sup>[7]</sup>, polyethyleneimine (PEI)/SiO<sub>2</sub> particles<sup>[8]</sup>, activated carbon microspheres<sup>[9, 10]</sup>, polymer granules<sup>[11]</sup>, and hydroxyapatite have been tested for their potential application to remove the excess uric acid<sup>[12]</sup>. Although their adsorption efficiencies are proved to be high, those adsorbents are weak in long adsorption time. In addition, all the studies have paid no attention to separate the adsorbents after uric acid adsorption. They are probably complicated in drawing out of the plasma. Therefore, a novel adsorbent which can realize fast and segregative removal of uric acid from plasma need to be developed.

---

\* Corresponding author: humphrey8531@hotmail.com  
<https://doi.org/10.15251/DJNB.2022.171.137>

Superparamagnetic iron oxide nanoparticles ( $\text{Fe}_3\text{O}_4$  NPs) are of good magnetic guidance for biomedical applications both *in vitro* [13] and *in vivo* [14] by external magnetism.  $\text{Fe}_3\text{O}_4$  NPs also have good performance on magnetic separation in biological nanomedicine [15]. It can be inferred that uric acid adsorbents based on  $\text{Fe}_3\text{O}_4$  NPs could be easily separated from plasma. On the other hand, biocompatible PEI has already been used for uric acid adsorption with high efficiency [18]. Herein, we have employed  $\text{Fe}_3\text{O}_4$  NPs as the core and PEI as the surface to fabricate the novel uric acid adsorbents for fast and segregative removal. Their adsorption efficiency and hemocompatibility have been investigated in this work.

## 2. Materials and methods

### 2.1. Materials

$\text{FeCl}_2 \cdot 4\text{H}_2\text{O}$  (Damao), hydrochloric acid (HCl), sodium hydroxide (NaOH), potassium nitrate ( $\text{KNO}_3$ ) (Chuangdong), PEI ( $M_w = 25000$ , Adamas-beta®), uric acid assay kits, BCA protein quantitation kits (Nanjing Jianchen), 3-(4,5-dimethylthiazol-2-yl)-2,5-diphenyltetrazolium bromide (MTT, Dingguo), RPMI-1640 (Hyclone), fetal bovine serum (FBS), trypsin (Gibco) were commercially available and used as received. Human umbilical vein endothelial cells (HUVEC) were purchased from ScienCell.

### 2.2. Synthesis of PEI-coated $\text{Fe}_3\text{O}_4$ NPs

0.729 g of NaOH and 2.046 g of  $\text{KNO}_3$  were dissolved in 150 mL of deionized water. Under  $\text{N}_2$  protection, HCl solution containing 0.331 g of  $\text{FeCl}_2 \cdot 4\text{H}_2\text{O}$  and 0.45 g of PEI was added dropwise under constant stirring. Then the mixture was held at 80 °C for 24 h, followed by an ice bath. The precipitation was collected by magnetic separation and washed three times with deionized water.

### 2.3. Characterization

The morphology of PEI-coated  $\text{Fe}_3\text{O}_4$  NPs was observed by scanning electron microscopy (SEM, SU-70 HITACHI). The Fourier transform infrared spectroscopy (FTIR) spectra were determined by Fourier transform infrared spectrometer (Spectrum GX Perkin Elmer). The zeta potential was determined by a dynamic light scattering instrument (Zetasizer Nano S90, Malvern). The magnetization value was determined by superconducting quantum interference device (MPMS-XL-7, Quantum Design).

### 2.4. Adsorption efficiency on uric acid of PEI-coated $\text{Fe}_3\text{O}_4$ NPs

Various mass of PEI-coated  $\text{Fe}_3\text{O}_4$  NPs (W:W=1:0.5, 1:1, 1:5, 1:25, 1:50, PEI-coated  $\text{Fe}_3\text{O}_4$  NPs:uric acid) were added into the high uric acid concentration plasma (above 420  $\mu\text{mol/L}$ ). Those mixtures were placed in a four-dimensional rotating mixer for 0.5 h. After that, magnetic separation was used to collect the supernatant. The residual uric acid and protein in the supernatant was determined by uric acid assay kits and BCA protein quantitation kits, respectively. All the experiments repeated thrice.

### 2.5. Hemocompatibility of PEI- $\text{Fe}_3\text{O}_4$ NPs

The hemolysis rate and thromboresistant ratio of PEI-coated  $\text{Fe}_3\text{O}_4$  NPs at 0.5 h with the above experimental concentrations were carried out to evaluate their hemocompatibility using the same processes as our previous work [14].

### 2.6. MTT proliferation assay

The HUVEC in their exponential growth phase were seeded into 96-well plates at a density of 5000 cells per well. After 12 h, PEI-coated  $\text{Fe}_3\text{O}_4$  NPs suspension with above concentrations were added into the culture medium. 0.5 h later, PEI-coated  $\text{Fe}_3\text{O}_4$  NPs were drawn out. MTT assay was used to determine the timely and 24 h's posterior cellular viability. All the experiments were repeated six times. The cells without any treatment were used as the positive control to set the cellular viability to 100%.

### 3. Results and discussion

PEI-coated  $\text{Fe}_3\text{O}_4$  NPs were prepared based on the commonly used oxidative hydrolysis method. Their morphology was observed by SEM (Fig. 1a). PEI-coated  $\text{Fe}_3\text{O}_4$  NPs were spherical and monodispersed. And their sizes were around 200 nm. The FTIR of PEI-coated  $\text{Fe}_3\text{O}_4$  NPs was shown in Fig. 1b. The adsorption peak around  $586\text{ cm}^{-1}$  resulted from Fe-O vibrations. And there were two intense bands at  $1630$  and  $3430\text{ cm}^{-1}$ , assigned to bending vibrations and stretching vibrations of N-H bond, respectively. These results indicated that PEI was successfully coated on the  $\text{Fe}_3\text{O}_4$  NPs. Meanwhile, the zeta potential of PEI-coated  $\text{Fe}_3\text{O}_4$  NPs had increased to  $48.5 \pm 9.2\text{ mV}$  due to the PEI coating. Primarily negative  $\text{Fe}_3\text{O}_4$  NPs<sup>[16]</sup> were surface-functionalized with abundant amino. So PEI-coated  $\text{Fe}_3\text{O}_4$  NPs became positive and stable. Fig. 1d showed the magnetization curve of PEI-coated  $\text{Fe}_3\text{O}_4$  NPs. The saturation of them was  $52.61\text{ emu/g}$ . The curve also demonstrated that PEI-coated  $\text{Fe}_3\text{O}_4$  NPs were superparamagnetic because there was no hysteresis and their remanence as well as coercivity were zero. And they could be easily gathered by external magnetism.

Superparamagnetism was essential for materials to realize facile magnetic separation<sup>[17-19]</sup>. It was well known that the shape and size of the nanoparticles greatly influenced their magnetic performance. Generally, the bigger size of magnetic core and the thinner coating of modified shell resulted in higher saturation magnetization<sup>[20]</sup>. Therefore, the size of magnetic adsorbents from plasma were bigger than  $100\text{ nm}$  to improve enough magnetic attraction<sup>[21-23]</sup>. The saturation of PEI-coated  $\text{Fe}_3\text{O}_4$  NPs of which size were around  $200\text{ nm}$  got as high as  $52.61\text{ emu/g}$ . This was close to that of those magnetic adsorbents used in substances removal from plasma<sup>[19]</sup> [23, 24]. In view of this, it was believable that PEI-coated  $\text{Fe}_3\text{O}_4$  NPs were able to easily be separate from plasma by magnetic separation.

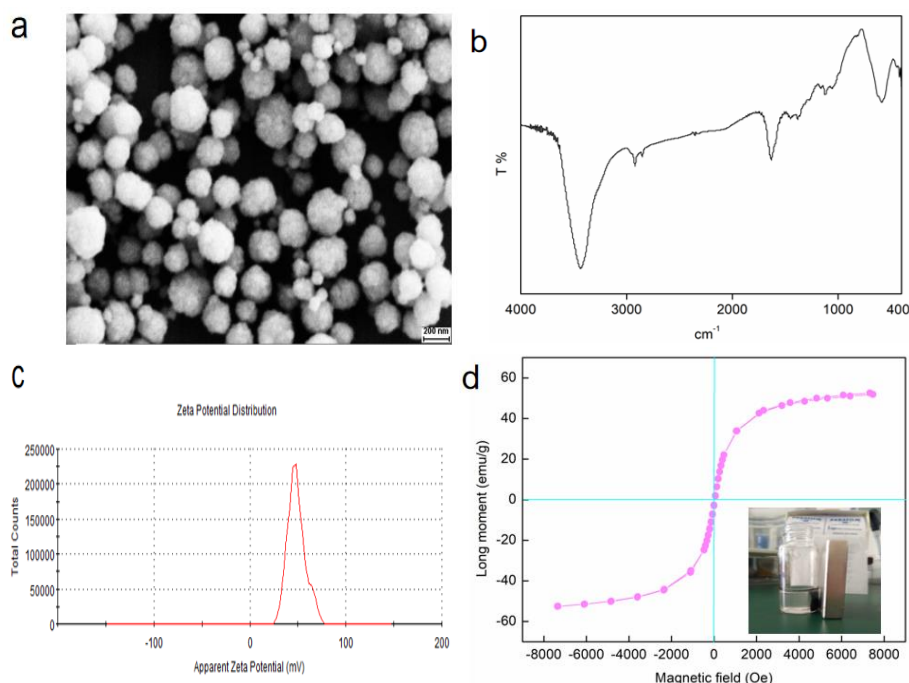


Fig. 1. Characterization. a SEM image; b FTIR; c Zeta potential; d Magnetic hysteresis loop.

Next, the adsorption efficiency on uric acid by PEI-coated  $\text{Fe}_3\text{O}_4$  NPs had been investigated. Fig. 2 showed the adsorption ratio. With the mass of PEI-coated  $\text{Fe}_3\text{O}_4$  NPs increased, more uric acid had been adsorbed. The uric acid adsorption behavior was in a concentration-dependent manner. When the ratio reached 1:1, more than 44% of uric acid had been adsorbed.

The adsorption quantity of uric acid on PEI-coated  $\text{Fe}_3\text{O}_4$  NPs was much larger than other adsorbents [8, 9, 11]. Although the removal ratio of PEI-coated  $\text{Fe}_3\text{O}_4$  NPs was lower than that of spherical carbonaceous adsorbent of which ratio approached 80%, the removal time of PEI-coated  $\text{Fe}_3\text{O}_4$  NPs was much shorter than that of spherical carbonaceous adsorbent of which time was 24 h [10]. This result indicated that PEI-coated  $\text{Fe}_3\text{O}_4$  NPs could become the fast and efficient uric acid adsorbents.

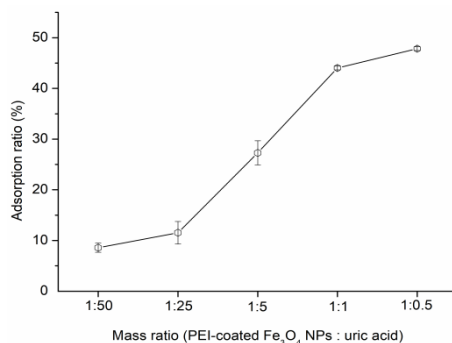


Fig. 2. The adsorption effect of uric acid by PEI-coated  $\text{Fe}_3\text{O}_4$  NPs.

After adsorption, the zeta potential of PEI-coated  $\text{Fe}_3\text{O}_4$  NPs decreased to  $-20 \pm 3.6$  mV (Fig. 3a). And, there no new intense band appeared in the FTIR except the spectra of PEI-coated  $\text{Fe}_3\text{O}_4$  NPs and uric acid (Fig. 3b). Positive PEI-coated  $\text{Fe}_3\text{O}_4$  NPs produced electrostatic interaction for negative uric acid. Therefore, the fast and efficient adsorption mainly depended on the electrostatic interaction.

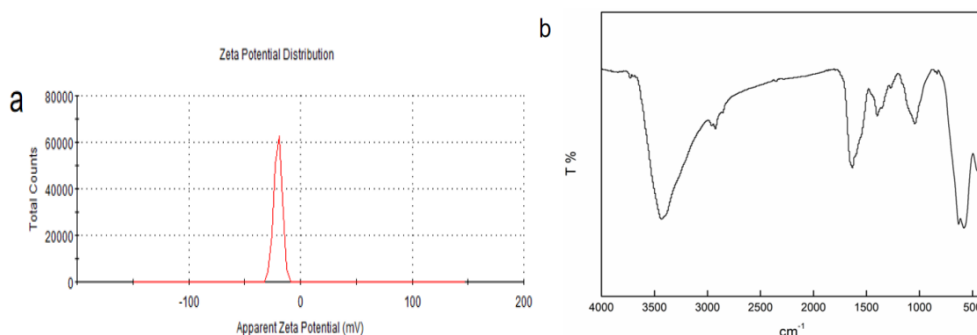


Fig. 3. The zeta potential (a) and FTIR (b) of PEI-coated  $\text{Fe}_3\text{O}_4$  NPs after uric acid adsorption.

In addition, BCA text was used to evaluate whether PEI-coated  $\text{Fe}_3\text{O}_4$  NPs adsorbed protein during the uric acid adsorption. Similarly, the adsorption behavior was also in a concentration-dependent manner. However, When the ratio was 1:1 ( $C_{\text{PEI-coated Fe}_3\text{O}_4 \text{ NPs}} = 70 \mu\text{g/mL}$ ), less than 10% protein had been adsorbed, of which amount was far below the adsorption amount of uric acid. The probable reason might be that uric acid with small molecular rapidly adhered to the surface of PEI-coated  $\text{Fe}_3\text{O}_4$  NPs, leaving little space to protein.

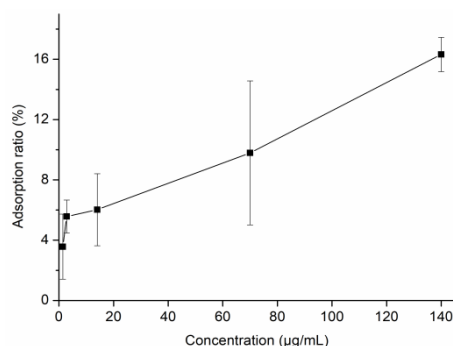


Fig. 4. The protein adsorption by PEI-coated Fe<sub>3</sub>O<sub>4</sub> NPs.

Since, PEI-coated Fe<sub>3</sub>O<sub>4</sub> NPs were expected to be used as a magnetic guided uric acid remover in blood vessels, their hemocompatibility and cytotoxicity to HUVEC were evaluated. Tab. 1 and Tab. 2 listed the hemolysis rates and thromboresistant ratios of PEI-coated Fe<sub>3</sub>O<sub>4</sub> NPs respectively. All the hemolysis rate were lower than 5%. It showed that PEI-coated Fe<sub>3</sub>O<sub>4</sub> NPs didn't cause hemolysis with those concentrations. Besides, PEI-coated Fe<sub>3</sub>O<sub>4</sub> NPs represented certain anticoagulant effect mainly because some clotting proteins had been adsorbed.

Table 1. Hemolysis rates of PEI-coated Fe<sub>3</sub>O<sub>4</sub> NPs.

Concentration (µg/mL)	Hemolysis rate (%)
1.40	0.13±0.05
2.80	0.21±0.07
14	0.78±0.09
70	1.28±0.14
140	1.63±0.12

Table 2. Thromboresistant ratios of PEI-coated Fe<sub>3</sub>O<sub>4</sub> NPs.

Concentration (µg/mL)	Thromboresistant ratio (%)
1.40	35.16±1.32
2.80	37.79±1.95
14	48.61±1.17
70	58.17±2.47
140	60.34±2.93

In addition, MTT test was performed to test the growth inhibition of various concentrations of PEI-coated Fe<sub>3</sub>O<sub>4</sub> NPs to HUVEC. The cellular viability at the end of adsorption was slightly lower than that of 24 h later. Except for the experimental group with the highest concentration, the viability of HUVEC in other experimental groups were all above 75% (Fig. 5). And those concentrations were deemed to be nearly no cytotoxicity [25]. Accordingly, PEI-coated Fe<sub>3</sub>O<sub>4</sub> NPs were not only hemocompatible but also cytocompatible under certain concentrations. Therefore, they could be a safe uric acid remover *in vivo*.

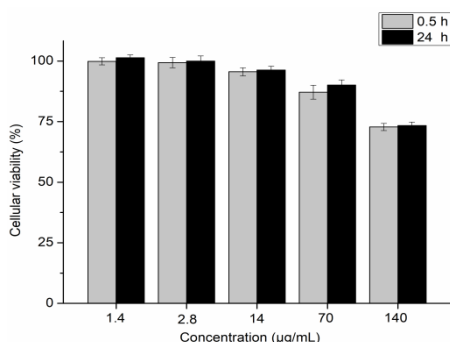


Fig. 5. Cytotoxicity of PEI-coated  $Fe_3O_4$  NPs.

#### 4. Conclusion

In conclusion, PEI-coated  $Fe_3O_4$  NPs have been used to adsorb excessive uric acid in plasma. They present a fast and efficient adsorption behavior. More importantly, PEI-coated  $Fe_3O_4$  NPs are superparamagnetic which can easily be separate from plasma by magnetic separation. In view of their good hemocompatibility and cytocompatibility, PEI-coated  $Fe_3O_4$  NPs hold a great potential in uric acid removal both *in vitro* and *in vivo*.

#### Acknowledgements

This work was funded by National Natural Science Foundation of China (81860324 & 31800839), Talent introduction project of Sichuan Institute of Technology (E10402600), High-level Innovative Talents in Guizhou Province (2018-2016-023).

#### References

- [1] N. S. Chaudhary, S. L. Bridges, K. G. Saag et al. *Hypertension* 75(1), 246 (2019); <https://doi.org/10.1161/HYPERTENSIONAHA.119.13580>
- [2] N. Dalbeth, H. K. Choi, L. A. B. Joosten et al., *Nature Reviews Disease Primers* 5(1), 1 (2019); <https://doi.org/10.1038/s41572-019-0115-y>
- [3] V. V. Fomin, T. E. Morosova, V. V. Tsurko. *Terapevticheskii Arkhiv* 91(12), 75 (2019); <https://doi.org/10.26442/00403660.2019.12.000173>
- [4] R. Li, Y. Kang, C. Li. *Asia Pacific Journal of Clinical Nutrition* 27, 1344 (2018).
- [5] S. Higa, D. Shima, N. Tomitani et al., *Journal of Clinical Hypertension* 21(9), 1713 (2019); <https://doi.org/10.1111/jch.13707>
- [6] R. Bao, M. Liu, D. Wang et al., *Frontiers in Pharmacology* 10, 1(2019); <https://doi.org/10.3389/fphar.2019.01464>
- [7] L. X. Zhang, M. Zhu, L. M. Guo et al., *Nano-Micro Letters* 1(001), 14 (2009); <https://doi.org/10.1007/BF03353599>
- [8] B. Gao, P. Jiang, H. Lei. *Materials Letters* 60(28), 3398 (2006); <https://doi.org/10.1016/j.matlet.2006.03.086>
- [9] X. Sun, Y. Tang, D. Di et al., *New Journal of Chemistry* 39(7), 5513 (2015); <https://doi.org/10.1039/C4NJ01777C>
- [10] M. T. Sultan, B. M. Moon, J. W. Yang et al., *Materials Science & Engineering C* 97, 55 (2019); <https://doi.org/10.1016/j.msec.2018.12.021>
- [11] A. P. Leshchinskaya, N. M. Ezhova, O. A. Pisarev, *Reactive and Functional Polymers* 102, 101 (2016); <https://doi.org/10.1016/j.reactfunctpolym.2016.02.014>

- [12] C. Zhang, Z. Xiao, T. Qin et al., *Journal of Saudi Chemical Society* 23(2), 249 (2019); <https://doi.org/10.1016/j.jscs.2018.11.009>
- [13] Z. Yu, Y. Guo, H. Dai et al., *Materials Express* 9(5), 467 (2019); <https://doi.org/10.1166/mex.2019.1525>
- [14] X. Huang, J. Lu, Y. Danyang et al., *Nanotechnology* 26(12), 1 (2015); <https://doi.org/10.1088/0957-4484/26/12/125101>
- [15] Y. Ma, T. Chen, M. Z. Iqbal et al., *Electrophoresis* 40(16-17), 2011 (2019); <https://doi.org/10.1002/elps.201800401>
- [16] P. Hernández, A. Lucero-Acuña, I. E. Moreno-Cortez et al., *Journal of Nanoscience and Nanotechnology* 20(4), 2063 (2020); <https://doi.org/10.1166/jnn.2020.17324>
- [17] S. Gauri, K. B. Gan, S.-M. Then, *Microsystem Technologies* 25(04), 1379 (2019); <https://doi.org/10.1007/s00542-018-4102-0>
- [18] H. M. Kim, D. M. Kim, C. Jeong et al., *Scientific Reports* 8, 1 (2018); <https://doi.org/10.1038/s41598-018-29948-9>
- [19] K. Du, X. Liu, S. Li et al., *ACS Sustainable Chemistry & Engineering* 6(9), 11578 (2018); <https://doi.org/10.1021/acssuschemeng.8b01699>
- [20] L. Kopanja, M. Tadić, S. Kralj et al., *Ceramics International* 44(11), 12340 (2018); <https://doi.org/10.1016/j.ceramint.2018.04.021>
- [21] L. Su, Y. Jin, Y. Huang et al., *Journal of Separation Science* 40(10), 2269 (2017); <https://doi.org/10.1002/jssc.201700080>
- [22] D. Jiang, T. Hu, H. Zheng et al., *Chemistry - An European Journal* 24(41), 10390 (2018); <https://doi.org/10.1002/chem.201800092>
- [23] Y. Zhang, M. Zhang, J. Yang et al., *Journal of Alloys & Compounds* 695, 3256 (2017); <https://doi.org/10.1016/j.jallcom.2016.11.239>
- [24] D. Jiang, X. Li, X. Lv et al., *Talanta* 185, 461(2018); <https://doi.org/10.1016/j.talanta.2018.04.006>
- [25] G. Ciapetti, E. Cenni, L. Pratelli et al., *Biomaterials* 14(5), 359 (1993); [https://doi.org/10.1016/0142-9612\(93\)90055-7](https://doi.org/10.1016/0142-9612(93)90055-7)